Strangeness Production in a Chemically Equilibrating Quark–Gluon Plasma

2004 Chinese Phys. Lett. 21 795

(http://iopscience.iop.org/0256-307X/21/5/009)

Strangeness Production in a Chemically Equilibrating Quark–Gluon Plasma *

HE Ze-Jun(贺泽君)[1,2,3**], LONG Jia-Li(龙家丽)[1], MA Yu-Gang(马余刚)[1,2], MA Guo-Liang(马国亮)[1]

[1] *Shanghai Institute of Applied Physics, Chinese Academy of Sciences, PO Box 800-204, Shanghai 201800*

[2] *CCAST (World Laboratory) PO Box 8730, Beijing 100080*

[3] *Research Centre of Nuclear Theory of National Laboratory of Heavy Ion Accelerator, Institute of Modern Physics, Chinese Academy of Sciences, Lanzhou 730000*

(Received 17 December 2003)

We study the strangeness of a chemically equilibrating quark–gluon plasma at finite baryon density based on the Jüttner distribution of partons. We find that the strangeness production depends obviously on the initial values, and will accelerate with the change of the initial system from a chemically non-equilibrated to an equilibrated system. We also find that the calculated strangeness is very different from the one in the thermodynamic equilibrium system. This study may be helpful to understand the formation of quark–gluon plasma via a chemically non-equilibrated evolution framework.

PACS: 12. 38. Mh, 25. 75. −q, 24. 85. +p

Many experiments are now underway at the relativistic heavy-ion collider (RHIC) at Brookhaven to study nuclear collisions at very high energies. The hope is to produce a deconfined quark–gluon plasma (QGP). Since QGP exists only for a very short time (several fm) in a small volume (about $100\,\mathrm{fm}^3$), a direct detection of this state of matter is not possible. Thus various indirect signatures have to be used for its detection, such as J/ψ suppression,[1] strangeness enhancement,[2] and dilepton spectra.[3−5]

Recently, researchers [6−8] have studied the evolution and dilepton production of a chemically equilibrating QGP system at finite baryon density. They have found that due to the increase of the quark phase lifetime with increasing initial quark chemical potential and other factors, such as higher initial temperature, larger gluon density, and gluon fusion or quark annihilation cross section, the system provides a significantly enhanced intermediate mass dilepton production. At the SPS energies, an enhanced production of strangeness, considered to be one of the more robust signatures of the quark–hadron phase transition, has been observed.[9−12] One naturally wonders how strangeness is produced and evolves in a chemically equilibrating QGP system created at RHIC energies. In order to answer these questions, we should include the dominant reactions leading to chemical equilibrium not only $gg \rightleftharpoons ggg$ and $gg \rightleftharpoons q\bar{q}$ but also $gg \rightleftharpoons s\bar{s}$ and $q\bar{q} \rightleftharpoons s\bar{s}$ in the system. Then, based on the Jüttner distribution function of partons for the Bjorken longitudinal scaling expansion from conservation laws of the energy–momentum and baryon number of the system, we derive a set of coupled relaxation equations governing evolutions of the temperature T, quark chemical potential μ_q and fugacities λ_q for quarks, λ_g for gluons and λ_s for s quarks. Finally, we solve the set of equations to calculate strangeness. It is worth emphasizing here the difference between our treatment and that of Ref. [13], in which the authors have taken the distribution function of partons as $f_j(E_j, \lambda_j) = \lambda_j f_j^{eq}(E_j)$, where $f_j^{eq}(E_j)$ is the thermodynamic equilibrium Bose–Einstein (Fermi–Dirac) distribution for gluons (quarks), and obviously have not considered the modification caused by the quark chemical potential in the strangeness production. Indeed, $f_j(E_j, \lambda_j)$ is the most commonly used approximation, as can be seen from the discussion in Ref. [14]. This approximation coincides with the Jüttner distribution only near $\lambda_g = 1$, however, and in the intermediate region of the λ_g the deviation is quite significant. We also mention that the authors of [15] have studied s quark production in the thermodynamic equilibrium QGP system. We shall compare our results with those calculated by formulae given in Ref. [15], and discuss the relation between our approach and that of Ref. [15]. In a thermodynamic equilibrium QGP system, strangeness production has also been studied on the basis of the relativistic hydrodynamic model in Ref. [16].

Considering the chemical potential of s quarks $\mu_s = 0$ since s quarks are created in pairs only, we first derive the thermodynamic relations of the chemically non-equilibrated system at finite baryon density. Expanding densities of quarks (anti-quarks) over quark chemical potential μ_q, we obtain the baryon density $n_{b,q}$ and the corresponding energy density including contribution from s quarks ε_{qgp}, as carried out in Ref. [6].

* Supported in part by the Knowledge Innovation Project of Chinese Academy of Sciences under Grant No KJCX2-N11, the National Natural Science Foundation of China under Grant Nos 10075071, 10135030, and 10328509, and the Major State Basic Research and Development Programme of China under Contract No G200077400

** Email: hezj@sinr.ac.cn

As mentioned above, we consider the reactions leading to chemical equilibrium $gg \rightleftharpoons ggg$, $gg \rightleftharpoons q\bar{q}$, $gg \rightleftharpoons s\bar{s}$ and $q\bar{q} \rightleftharpoons s\bar{s}$. Provided that elastic parton scatterings are sufficiently rapid to maintain local thermal equilibrium, the evolutions of gluon, quark and s quark density can be given by the following master equations, according to the line of Refs. [14,17], respectively:

$$\begin{aligned}\partial_\mu(n_g u^\mu) = {} & R_3 n_g\Big[1-\frac{n_g}{\bar{n}_g}\Big] \\ & - 2R_2^{g-q} n_g\Big[1-\Big(\frac{\bar{n}_g}{n_g}\Big)^2\frac{n_q n_{\bar{q}}}{\bar{n}_q\bar{n}_{\bar{q}}}\Big] \\ & - 2R_2^{g-s} n_g\Big[1-\Big(\frac{\bar{n}_g}{n_g}\Big)^2\frac{n_s n_{\bar{s}}}{\bar{n}_s\bar{n}_{\bar{s}}}\Big],\end{aligned} \tag{1}$$

$$\begin{aligned}\partial_\mu(n_q u^\mu) = {} & R_2^{g-q} n_g\Big[1-\Big(\frac{\bar{n}_g}{n_g}\Big)^2\frac{n_q n_{\bar{q}}}{\bar{n}_q\bar{n}_{\bar{q}}}\Big] \\ & - 2R_2^{q-s} n_q\Big[1-\Big(\frac{\bar{n}_q}{n_q}\Big)^2\frac{n_s n_{\bar{s}}}{\bar{n}_s\bar{n}_{\bar{s}}}\Big],\end{aligned} \tag{2}$$

and

$$\begin{aligned}\partial_\mu(n_s u^\mu) = {} & R_2^{g-s} n_g\Big[1-\Big(\frac{\bar{n}_g}{n_g}\Big)^2\frac{n_s n_{\bar{s}}}{\bar{n}_s\bar{n}_{\bar{s}}}\Big] \\ & + R_2^{q-s} n_q\Big[1-\Big(\frac{\bar{n}_q}{n_q}\Big)^2\frac{n_s n_{\bar{s}}}{\bar{n}_s\bar{n}_{\bar{s}}}\Big].\end{aligned} \tag{3}$$

Considering that taking $\lambda_q = \lambda_{\bar{q}}$ does not change the qualitative property of the evolution of the system because the calculated initial quark chemical potential for $A_u^{197}+A_u^{197}$ collisions at RHIC energies is relatively small, combining these master equations together with equations of baryon number and energy–momentum conservation

$$\partial_\mu(n_{b,q}u^\mu) = 0, \tag{4}$$

$$\frac{\partial\varepsilon_{qgp}}{\partial\tau} + \frac{\varepsilon_{qgp}+P}{\tau} = 0, \tag{5}$$

we obtain a set of coupled relaxation equations. Here $n_{s(\bar{s})}$, n_g, $n_{q(\bar{q})}$, $n_{b,q}$ are, respectively, the number densities of s quark (s anti-quark), gluon, quark (anti-quark) and baryon; ε_{qgp} is the energy density, and p the momentum of the system. These have been given in Ref. [6]. For the longitudinal scaling expansion of the system, we solve this set of equations to obtain the evolutions of temperature T, quark chemical potential μ_q and fugacities λ_q for quarks, λ_g for gluons and λ_s for s quarks, where $\bar{n}_{q(\bar{q})}$ is the value of $n_{q(\bar{q})}$ at $\lambda_{q(\bar{q})} = 1$, $n_q^0 = n_q/(g_q/2\pi^2)$, $n_g^0 = n_g/(g_g/2\pi^2)$, $\xi(3) = 1.20206$. Adopting factorizations as done in Refs. [6,14,17,18], finally, we have production rates for processes $gg \to ggg$, $gg \to q\bar{q}$ and $gg \to \bar{s}s$:

$$\frac{R_3}{T} = \frac{32}{3a_1}\frac{\alpha_s}{\lambda_g}\Big[\frac{(M_D^2+s/4)M_D^2}{9g^2T^4/2}\Big]^2 I(\lambda_g,\lambda_q,T,\mu_q), \tag{6}$$

$$\frac{R_2^{g-q}}{T} = \frac{g_g}{24\pi}\frac{G_1^{1^2}}{G_1^2}N_f\alpha_s^2\lambda_g\ln(1.65/\alpha_s\lambda^q), \tag{7}$$

$$\frac{R_2^{g-s}}{T} = \frac{g_g}{24\pi}\frac{G_1^{1^2}}{G_1^2}N_f\alpha_s^2\lambda_g\ln(1.65/\alpha_s\lambda^s), \tag{8}$$

$$M_D^2 = \frac{3g^2T^2}{\pi^2}\Big[2G_1^1\lambda_g + 2N_f Q_1^1\lambda_q + \Big(\frac{\mu_q}{T}\Big)^2\Big(\frac{\lambda_q}{\lambda_q+1}\Big)\Big], \tag{9}$$

with

$$\lambda^q = \lambda_g + \frac{1}{G_1^1}\Big[Q_1^1\lambda_q + \Big(\frac{\mu_q}{T}\Big)^2\Big(\frac{\lambda_q}{\lambda_q+1}\Big)\Big], \tag{10}$$

$$\lambda^s = \lambda_g + \frac{1}{G_1^1}S_1^1\lambda_s, \tag{11}$$

and the running coupling constant $\alpha_s(T) = 6\pi/27\ln[T/(50\,\mathrm{MeV})]$, where M_D^2 is the Debye screening mass, $a_1 = g_g 2\pi^2 G_1^2$, $I(\lambda_g,\lambda_q,T,\mu_q)$ the function of λ_g, λ_q, T, μ_q,[18] and N_f the quark flavour. G_1^1 and G_1 are integral factors appearing in the expansion.[6] Similarly, the production rate R_2^{q-s}/T for process $q\bar{q} \to s\bar{s}$ is obtained via taking cross section $\sigma(q\bar{q} \to s\bar{s})$ from Ref. [19].

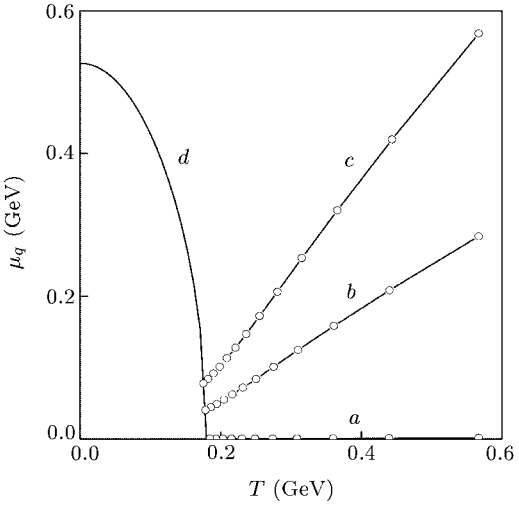

Fig. 1. The calculated evolution paths of the system in the phase diagram for initial values $\tau_0 = 0.70\,\mathrm{fm}$, $T_0 = 0.57\,\mathrm{GeV}$, $\lambda_{g0} = 0.09$, $\lambda_{q0} = 0.02$ and $\lambda_{s0} = 0.01$, where curves a, b and c are, in turn, the evolution paths for initial quark chemical potentials $\mu_{q0} = 0.000$, 0.284 and $0.568\,\mathrm{GeV}$, and the curve d is the phase boundary of the phase diagram. The time interval between the two small circles is $0.3\,\mathrm{fm}$ (i.e. $30\times$ calculation-step $0.01\,\mathrm{fm}$). The phase diagram is calculated at $B^{1/4} = 0.25\,\mathrm{GeV}$.

From perturbative QCD within the Glauber multiple scattering theory for $\sqrt{s} = 200\,\mathrm{A\,GeV}$, the authors in Ref. [20] have obtained the energy density and number densities of gluons, quarks and anti-quarks as well as the initial temperature $T_0 = 0.552\,\mathrm{GeV}$. From these densities we have also obtained the initial temperature $T_0 = 0.566\,\mathrm{GeV}$ and the initial quark chemical potential $\mu_{q0} = 0.284\,\mathrm{GeV}$ based on thermodynamic

relations of the chemically equilibrating system with finite baryon density, derived by us, at $\lambda_{g0} = 0.09$ and $\lambda_{q0} = 0.02$. With the help of Ref. [12], finally we have taken the initial values: $\tau_0 = 0.70\,\mathrm{fm}$, $T_0 = 0.57\,\mathrm{GeV}$, $\lambda_{g0} = 0.09$, $\lambda_{q0} = 0.02$ and $\lambda_{s0} = 0.01$, and solved the set of coupled relaxation equations for the initial quark chemical potentials $\mu_{q0} = 0.000$, 0.284 and 0.568 GeV. The calculated evolution paths in the phase diagram are shown in Fig. 1, in which curves *a*–*c* denote the calculated paths for initial quark chemical potentials $\mu_{q0} = 0.000$, 0.284 and 0.568 GeV, respectively; curve *d* represents the phase boundary between the quark phase and the hadronic phase.

It is known that baryon-free QGP converts into hadronic matter only with decreasing temperature along the temperature axis of the phase diagram, and the phase transition occurs at a certain critical temperature T_c. However, in this work, both the quark chemical potential and the temperature of the system are functions of time; compared with the baryon-free QGP it necessarily takes a long time for value (μ_q, T) of the system to reach a certain point of the phase boundary to make the phase transition. Such an effect will cause increase of the lift-time of the quark phase. Furthermore, we have found that with the increasing initial quark chemical potential, the production rate R_3/T of gluons increases and the gluon equilibration rate necessarily decreases,[6] thus leading to the small energy consumption of the system, i.e. slow cooling of the system. Since gluons are much more numerous than quarks in the system, overall with the increasing initial quark chemical potential, the cooling of the system further slows down. The calculated presence times of the system in the quark phase for initial values $\mu_q = 0.000$, 0.284 and 0.568 GeV are, in turn, about 3.57, 3.76, and 3.95 fm. Compared to those values calculated in Ref. [6], one can see that due to inclusion of reactions $gg \to \bar{s}s$ and $\bar{q}q \to \bar{s}s$, the energy consumption of the system becomes even faster leading to some increase of the cooling rate of the system. We have marked an equal time step on the paths in Fig. 1. The time interval between the two small circles is 0.30 fm (i.e. 30× calculation-step 0.01 fm). We can clearly see that the evolution of the system becomes progressively slower with increase of the evolution time.

We have calculated the chemical equilibration rate of *s* quarks via taking initial values $\tau_0 = 0.7\,\mathrm{fm}$, $T_0 = 0.57\,\mathrm{GeV}$, $\lambda_{g0} = \lambda_{q0} = 1$ (i.e. in a chemically equilibrated QGP system), $\lambda_{s0} = 0.01$ and $\mu_{q0} = 0.284\,\mathrm{GeV}$. The calculated result is shown by curve *b* in Fig. 2. Curve *a* is obtained for the initial values $\tau_0 = 0.7\,\mathrm{fm}$, $T_0 = 0.57\,\mathrm{GeV}$, $\lambda_{g0} = 0.09$, $\lambda_{q0} = 0.02$, $\lambda_{s0} = 0.01$ and $\mu_q = 0.284\,\mathrm{GeV}$. The set of coupled relaxation equations governs the system to tend to the chemical equilibrium, i.e. $\lambda_g = \lambda_q = \lambda_s = 1$. After quarks and gluons reach chemical equilibrium, only a few quarks and gluons can join chemical reactions during the evolution, thus the corresponding rates λ_q and λ_g have to adopt the evolution as shown by curves *c* and *d* in Fig. 2, respectively, causing the *s* quark production rate to decrease and the chemical equilibration rate to increase rapidly. Thus, we can see that in Fig. 2, λ_s shown by curve *b* rises much more rapidly

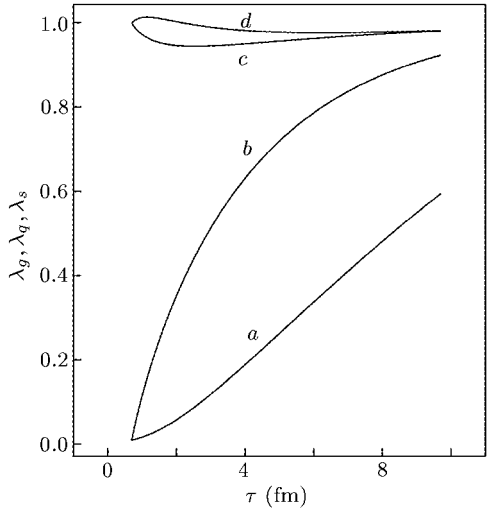

Fig. 2. Calculated chemical equilibration rate of *s* quarks at the quark and gluon chemically equilibrated system (i.e. $\lambda_{g0} = \lambda_{g0} = 1$) for initial values $\tau_0 = 0.7\,\mathrm{fm}$, $T_0 = 0.57\,\mathrm{GeV}$, $\mu_{s0} = 0.284\,\mathrm{GeV}$ and $\lambda_{s0} = 0.01$. Curves *b*, *c* and *d* are, respectively, the calculated equilibration rates of λ_s, λ_q and λ_g, while curve *a* is the calculated *s* quark equilibration rate for the initial values as given in Fig. 1 and at $\mu_{s0} = 0.284\,\mathrm{GeV}$.

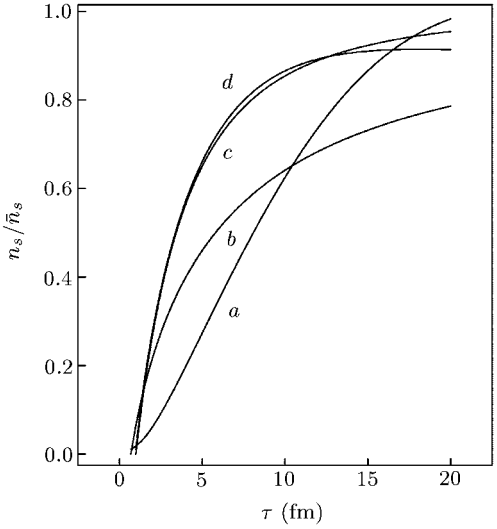

Fig. 3. Calculated strangeness $n_s/\bar{n}_s$. Curve *a* is the calculated value for the same initial values as given in Fig. 2, curve *d* for the initial values $\lambda_{g0} = \lambda_{q0} = 1.00$, and $\lambda_{s0} = 0.01$ at $\tau_0 = 1.00\,\mathrm{fm}$. In addition, curves *b* and *c* are the calculated values in the thermodynamic equilibrium system [13] for the initial values $\tau_0 = 0.7$ and 1.0 fm at $n_s(\tau_0) = 0$, respectively.

with the increasing evolution time than that shown by curve a. This shows that the chemical equilibration of strangeness depends obviously on the initial system.

We have calculated the strangeness $n_s/\bar{n}_s$ according to the relation

$$n_s = \frac{g_s T^3}{2\pi^2} \int \frac{\lambda_s Z^2 dZ}{e^{[Z^2+(m_s/T)^2]^{1/2}} + \lambda_s}, \qquad (12)$$

where $\bar{n}_s$ is the value of n_s at $\lambda_s = 1$, and $Z = p/T$. In Fig. 3, curves a and d are, respectively, the calculated strangeness for the two sets of initial values: $\tau_0 = 0.70\,\mathrm{fm}$, $T_0 = 0.57\,\mathrm{GeV}$, $\lambda_{g0} = 0.09$, $\lambda_{q0} = 0.02$ and $\lambda_{s0} = 0.01$; $\tau_0 = 1.00\,\mathrm{fm}$, $T_0 = 0.57\,\mathrm{GeV}$, $\lambda_{g0} = \lambda_{q0} = 1$ and $\lambda_{s0} = 0.01$ as used above. Since at the initial values $\lambda_{g0} = \lambda_{q0} = 1$, the equilibration rate λ_s increases even more rapidly with evolution time, as shown in Fig. 2. Moreover, Eq. (12) shows that the strangeness is directly proportional to the equilibration rate λ_s; one can see that curve d rises much more rapidly than curve a. Curves b and c are obtained in the thermodynamic equilibrium QGP system as described in Ref. [13] at $\tau_0 = 0.7$ and $1.0\,\mathrm{fm}$ for $n_s(\tau_0) = 0$, respectively. One can note that in Fig. 3, curve d coincides with curve c in the region we are interested in. This shows that the strangeness evolution in the system with the initial values $\tau_0 = 1.00\,\mathrm{fm}$, $T_0 = 0.57\,\mathrm{GeV}$, $\lambda_{g0} = \lambda_{q0} = 1$ and $\lambda_{s0} = 0.01$ is almost the same as that obtained in the thermodynamic equilibrium system [13] at $\tau_0 = 1.0\,\mathrm{fm}$, $T_0 = 0.57\,\mathrm{GeV}$, and $n_s(\tau_0) = 0$. We also find from Fig. 3 that the strangeness evolution in the chemically equilibrating system is very different from the one in the chemically equilibrated system.

In conclusion, the present framework may also approach the strangeness production in the thermodynamic equilibrium QGP system, qualitatively, therefore based on this framework we may study the strangeness production in the whole evolution process from the chemically non-equilibrated to equilibrated QGP. In particular, the calculated strangeness in the thermodynamic equilibrium QGP is very different from the one in the chemically equilibrating QGP. It is very significant to study strangeness in the chemically equilibrating QGP, and it may be helpful to look for signatures of the QGP formation and to explore the thermodynamic properties of the QGP.

References

[1] Matsui T and Satz H 1986 *Phys. Lett.* B **178** 416
[2] Rafelski J and Müller B 1982 *Phys. Rev. Lett.* **48** 1066
[3] Shuryak E 1980 *Phys. Rep.* **80** 71
[4] Kajantie K, Kapusta J, McLerran L and Mekjian A 1986 *Phys. Rev.* D **34** 2746
[5] Dumitru A, Rischke D H and Schönfeld Th et al 1993 *Phys. Rev. Lett.* **70** 2860
[6] He Z J, Long J L, Jiang W Z, Ma Y G and Liu B 2003 *Phys. Rev.* C **68** 042902-1
[7] He Z J et al 2003 *Chin. Phys. Lett.* **21** 47
[8] Long J L et al 2004 *Chin. Phys. Lett.* 20 836
[9] Gyulassy M 1984 *Nucl. Phys.* A **418** 594c
[10] Matsui T, Svetitsky B and McLerran L D 1986 *Phys. Rev.* D **34** 783
[11] Geiger K 1993 *Phys. Rev.* D **48** 4129
[12] Letessier J and Rafelski J 2000 *Nucl. Phys.* A **661** 497c
[13] Pal D, Sen A and Mustafa M G 2002 *Phys. Rev.* C **65** 034901-1
[14] Biró T S, Doorn E V, Müller B et al 1993 *Phys. Rev.* C **48** 1275
[15] Kapusta J and Mekjian A 1986 *Phys. Rev.* D **33** 1304
[16] He Z J, Zhang J J and Zhou B S 1993 *J. Phys.* G **19** L7
[17] Lévai P, Müller and Wang X N 1995 *Phys. Rev.* C **51** 3326
[18] Eskola K J, üller B and Wang X N 1996 *Phys. Lett.* B **374** 20
[19] Combridge B L 1979 *Nucl. Phys.* B **151** 429
[20] Hammon N, Stöcker H, and Greiner W 1999 *Phys. Rev.* C **61** 014901-1